METABOLIC DISORDERS

Recombinant porphobilinogen deaminase targeted to the liver corrects enzymopenia in a mouse model of acute intermittent porphyria

Karol M. Córdoba[1,2]†, Irantzu Serrano-Mendioroz[1,2]†, Daniel Jericó[1,2], María Merino[3], Lei Jiang[4], Ana Sampedro[1,2], Manuel Alegre[5], Fernando Corrales[6], María J. Garrido[3], Paolo G. V. Martini[4], José Luis Lanciego[2,7,8], Jesús Prieto[1]*‡, Pedro Berraondo[2,9,10]‡, Antonio Fontanellas[1,2,11]*‡

Correction of enzymatic deficits in hepatocytes by systemic administration of a recombinant protein is a desired therapeutic goal for hepatic enzymopenic disorders such as acute intermittent porphyria (AIP), an inherited porphobilinogen deaminase (PBGD) deficiency. Apolipoprotein A-I (ApoAI) is internalized into hepatocytes during the centripetal transport of cholesterol. Here, we generated a recombinant protein formed by linking ApoAI to the amino terminus of human PBGD (rhApoAI-PBGD) in an attempt to transfer PBGD into liver cells. In vivo experiments showed that, after intravenous injection, rhApoAI-PBGD circulates in blood incorporated into high-density lipoprotein (HDL), penetrates into hepatocytes, and crosses the blood-brain barrier, increasing PBGD activity in both the liver and brain. Consistently, the intravenous administration of rhApoAI-PBGD or the hyperfunctional rApoAI-PBGD-I129M/N340S (rApoAI-PBGDms) variant efficiently prevented and abrogated phenobarbital-induced acute attacks in a mouse model of AIP. One month after a single intravenous dose of rApoAI-PBGDms, the protein was still detectable in the liver, and hepatic PBGD activity remained increased above control values. A long-lasting therapeutic effect of rApoAI-PBGDms was observed after either intravenous or subcutaneous administration. These data describe a method to deliver PBGD to hepatocytes with resulting enhanced hepatic enzymatic activity and protection against AIP attacks in rodent models, suggesting that the approach might be an effective therapy for AIP.

INTRODUCTION

Acute intermittent porphyria (AIP; Mendelian Inheritance in Man: 176000) is a rare metabolic disorder caused by autosomal dominant loss-of-function mutations of porphobilinogen deaminase (PBGD; enzyme commission number 2.5.1.61), the third enzyme of the heme biosynthesis pathway. Heme controls its own synthesis by modulating the expression of δ-aminolevulinate synthase 1 (*ALAS1*), the first enzyme of the pathway. In patients with AIP, factors that activate heme biosynthesis, such as fasting, hormones, and certain drugs, strongly up-regulate ALAS1, leading to accumulation of the heme precursors, δ-aminolevulinate (ALA) and porphobilinogen (PBG), and the associated occurrence of acute neurovisceral attacks. These are characterized by abdominal pain, hypertension, nausea, vomiting, anxiety, insomnia, and, occasionally, motor neuropathy, which may progress to tetraplegia (*1*, *2*). About 5% of patients suffer a devastating form of the disease with frequent and severe attacks, seriously affecting their life quality (*1*, *2*).

Treatment of acute attacks relies on intravenous hemin infusion, which initiates a feedback inhibition of *ALAS1* and reduction of ALA and PBG production. However, the benefit of hemin is short-lived and its repeated use is associated with side effects such as phlebitis and iron overload (*3*, *4*). Recently, givosiran, an RNA interference agent targeting hepatic *ALAS1* mRNA, has received U.S. Food and Drug Administration approval for the prevention of porphyric attacks. However, this emerging therapy does not normalize heme stores and may increase the risk of hepatic and renal adverse events (*5*–*8*). With the aim of enhancing hepatic PBGD expression, liver-directed gene therapy has been tried in patients with severe porphyria using an adeno-associated virus serotype 5 (AAV5) vector encoding PBGD. This treatment was well tolerated but did not achieve correction of the enzymatic defect, likely due to insufficient liver transduction (*9*). More recently, the use of lipid nanoparticles containing mRNA encoding PBGD has been shown to restore hepatic enzymatic activity in AIP mice (*10*). In addition, enzyme replacement therapy has been attempted using intravenous administration of rhPBGD. However, the half-life of this protein is very short and the clinical trial performed to test its therapeutic value was promptly interrupted due to lack of efficacy (*11*). Orthotopic liver transplantation represents a curative strategy; however, it is costly and advanced pretransplant neurological impairment and diminished renal function increase the risk for poor outcomes (*12*).

In this work, we aimed to increase hepatic PBGD activity in AIP mice using a recombinant PBGD protein targeted to the liver. As apolipoprotein A-I (ApoAI) is an integral part of high-density lipoprotein (HDL), a lipoprotein that mediates the centripetal transport of cholesterol from periphery to the liver (*13*), and ApoAI receptors

[1]Hepatology Program, Center for Applied Medical Research (CIMA), University of Navarra, 31008 Pamplona, Spain. [2]Navarra Institute for Health Research (IDISNA), 31008 Pamplona, Spain. [3]Department of Pharmacy and Pharmaceutical Technology, School of Pharmacy, University of Navarra, 31008 Pamplona, Spain. [4]Moderna Inc., Cambridge, MA 02139, USA. [5]Neurophysiology Laboratory, Neuroscience Area, CIMA and Clínica Universitaria, University of Navarra, 31008 Pamplona, Spain. [6]Proteomics Unit, Centro Nacional de Biotecnología (CSIC), 28049 Madrid, Spain. [7]Neurosciences Department, CIMA-University of Navarra, 31008 Pamplona, Spain. [8]Centro de Investigación Biomédica en Red de Enfermedades Neurodegenerativas (CIBERNed), Instituto de Salud Carlos III, 28031 Madrid, Spain. [9]Program of Immunology and Immunotherapy, Cima Universidad de Navarra, 31008 Pamplona, Spain. [10]Centro de Investigación Biomédica en Red de Cáncer (CIBERONC), Instituto de Salud Carlos III, 28029 Madrid, Spain. [11]Centro de Investigación Biomédica en Red de Enfermedades Hepáticas y Digestivas (CIBERehd), Instituto de Salud Carlos III, 28029 Madrid, Spain.
*Corresponding author. Email: afontanellas@unav.es (A.F.); jprieto@unav.es (J.P.)
†These authors contributed equally to this work.
‡These authors jointly supervised this work.

are highly expressed by parenchymal liver cells (*14*), we reasoned that binding PBGD to ApoAI could promote internalization of the enzyme into hepatocytes. Here, we tested the efficacy of ApoAI bound to PBGD to treat a well-characterized murine model of AIP.

RESULTS

Pharmacokinetics and pharmacodynamics of the recombinant proteins

We produced two recombinant ApoAI-conjugated PBGD molecules, with human ApoAI either at the N or C terminus of human PBGD (rhApoAI-PBGD and rhPBGD-ApoAI, respectively). AIP mice were injected intravenously with rhApoAI-PBGD, rhPBGD-ApoAI, or unconjugated rhPBGD (60 nmol/kg). We observed that rhPBGD was short-lived in the circulation (half-life of 0.75 hours), whereas the other two molecules persisted in serum for an extended period of time ($P < 0.001$), where the half-life of rhApoAI-PBGD and rhPBGD-ApoAI is 9.9 and 7.5 hours, respectively (Fig. 1A).

As ApoAI is a key component of HDL, we investigated whether rhApoAI-PBGD circulates incorporated into these particles. Therefore, we performed Western blot analysis of lipoprotein fractions obtained from the serum of AIP mice that had received an intravenous injection of rhApoAI-PBGD (60 nmol/kg) 72 hours previously. The immunoblot probed with anti-PBGD revealed a conspicuous band in the HDL fraction corresponding to the molecular weight of rhApoAI-PBGD (68 kDa) and that was absent in low-density and very low density lipoproteins (LDL and VLDL, respectively) (Fig. 1B). In contrast, in the HDL fraction, anti-ApoAI detected the endogenous ApoAI band at 28 kDa and two other bands at 68 and 66 kDa corresponding to rhApoAI-PBGD and a partially proteolyzed product. In agreement with these observations, measurable PBGD enzymatic activity was found in the HDL fraction of AIP mice 72 hours after dosing with rhApoAI-PBGD, whereas no PBGD activity was present in HDL from mice given rhPBGD 36 hours previously (Fig. 1C).

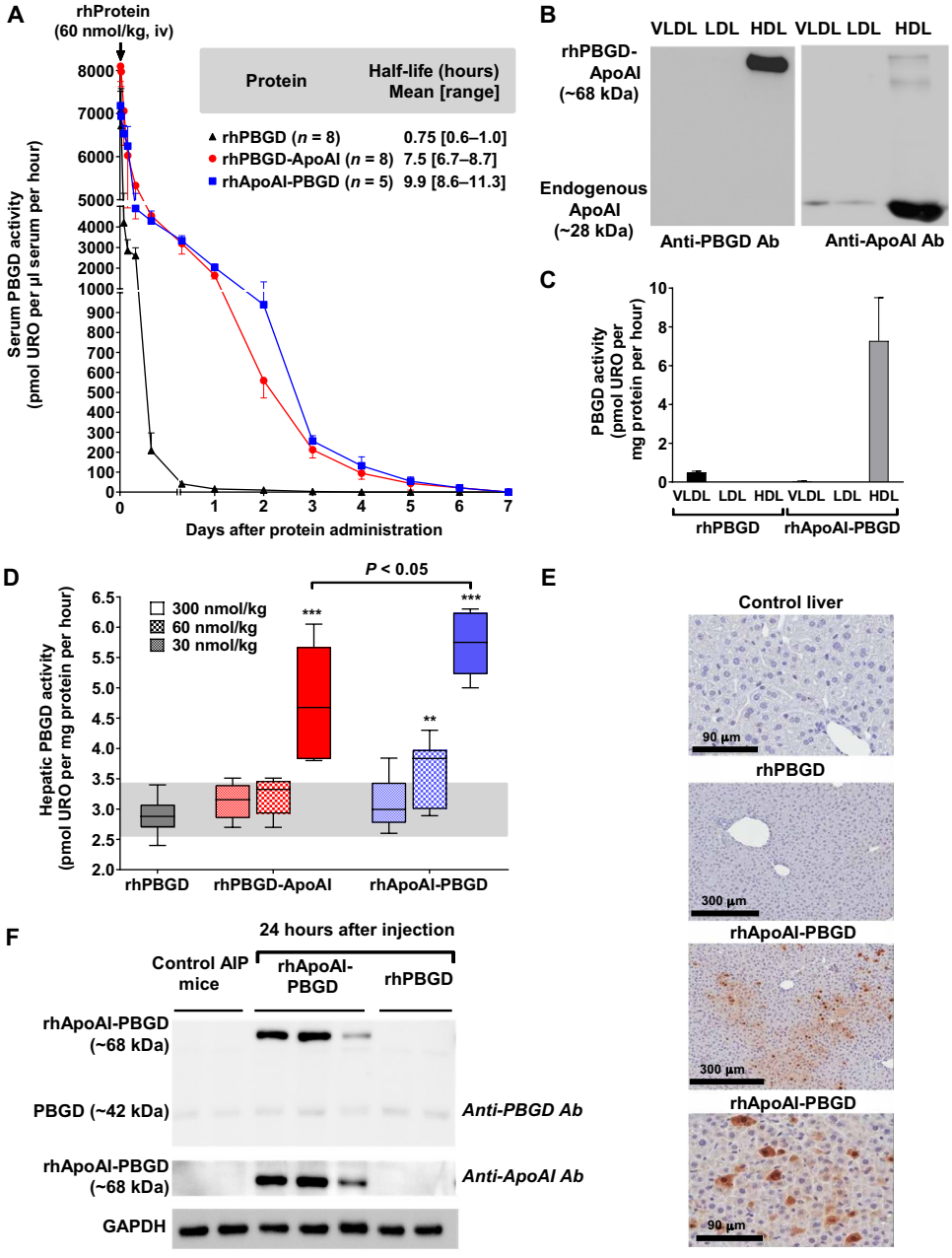

Fig. 1. Long half-life of rhApoAI-PBGD in circulation, its transport by HDL, and liver targeting. (**A**) Pharmacokinetic study of rhPBGD, rhPBGD-ApoAI, and rhApoAI-PBGD in AIP mice after intravenous (iv) injection of these proteins (60 nmol/kg). (**B**) Immunoblot detection of PBGD and ApoAI, and (**C**) PBGD enzymatic activity in lipoprotein fractions from mice 72 hours after dosing with rhApoAI-PBGD (60 nmol/kg) or with the same dose of rhPBGD 36 hours after dosing (mean of two independent experiments with $n = 3$ each). Ab, antibody. (**D**) Hepatic PBGD activity in AIP mice 24 hours after intravenous administration of saline, rhPBGD (300 nmol/kg), or rhPBGD-ApoAI or rhApoAI-PBGD (30, 60, or 300 nmol/kg). Gray box corresponds to means ± 2× SD of saline control group. $^{**}P < 0.01$ and $^{***}P < 0.001$ versus rhPBGD group. (**E**) Immunohistochemical detection of PBGD in liver samples from untreated AIP mouse and mouse 24 hours after dosing with rhPBGD or rhApoAI-PBGD (300 nmol/kg). (**F**) Western blot of liver specimens from AIP mice sacrificed 24 hours after intravenous injection of rhPBGD or rhApoAI-PBGD (300 nmol/kg).

We then analyzed whether the linkage of PBGD to ApoAI enabled transferring the enzyme to the liver tissue. Female AIP mice were treated with intravenous injection of rhApoAI-PBGD or rhPBGD-ApoAI (30, 60, or 300 nmol/kg), and liver samples were taken 24 hours after injection. The administration of these compounds caused a dose-related increase of hepatic PBGD enzymatic activity. In contrast, rhPBGD given intravenously at the highest dose (300 nmol/kg) did not modify hepatic PBGD activity when compared to animals given

saline (Fig. 1D). rhApoAI-PBGD increased hepatic enzymatic activity more than rhPBGD-ApoAI, and accordingly, the former was selected for subsequent studies.

In line with these findings, immunochemical detection of PBGD in liver samples taken from AIP mice 24 hours after intravenous injection of rhApoAI-PBGD (300 nmol/kg) showed the presence of areas of hepatocytes (mainly around centrilobular veins), exhibiting positive staining, whereas untreated animals or treated with the same dose of rhPBGD showed no positivity (Fig. 1E and fig. S1). Positive areas were 0% in the liver of control and rhPBGD-injected mice, and 3.24% and 9.01% in the liver of mice injected with rhApoAI-PBGD, at resolutions of 300 and 90 μm, respectively (Fig. 1E). Consistent with this observation, PBGD immunoblots of liver tissue collected 24 hours after intravenous administration of rhApoAI-PBGD (300 nmol/kg) revealed the presence of a strong band of 68 kDa corresponding to the molecular size of rhApoAI-PBGD, and no signal was observed in those mice treated with an equal dose of rhPBGD [Fig. 1F; rhApoAI-PBGD/endogenous PBGD ratio of 0.0 ± 0.06 in control and rhPBGD-mice versus 14.9 ± 7.6 in animals injected with rhApoAI-PBGD, $P < 0.05$ with anti-PBGD antibody; rhApoAI-PBGD/glyceraldehyde-3-phosphate dehydrogenase (GAPDH) ratio of 0.0 ± 0.04 in control and mice inoculated with rhPBGD versus 1.1 ± 0.4 in animal injected with rhApoAI-PBGD, $P < 0.05$]. The 68-kDa band was still present in livers from mice sacrificed 3 and 5 days after administering rhApoAI-PBGD, indicating prolonged persistence of the conjugated protein in the hepatic tissue [fig. S2; rhApoAI-PBGD/endogenous PBGD ratio of 0 ± 0 in control and mice injected with rhPBGD versus 1.5 ± 0.01 ($P < 0.001$) and 0.9 ± 0.02 ($P < 0.01$) in rhApoAI-PBGD–injected animals on days 3 and 5, respectively].

Next, the stability of PBGD linked to ApoAI within liver cells was evaluated, as compared to unconjugated PBGD. For this purpose, liver parenchymal cells of AIP mice were transfected with mRNA encoding ApoAI-PBGD or PBGD formulated in lipid nanoparticles, a technology previously described that transiently expresses the protein of interest into the hepatocytes (*10*). Some animals were sacrificed 24 hours after the administration of lipid nanoparticles to confirm that hepatic PBGD activity was similar in both groups of treated AIP mice (fig. S3A). Mice were then subjected to two phenobarbital challenges: the first between days 1 and 4 after therapy and the second between days 12 and 15. During the first challenge, both groups were similarly protected against the accumulation of porphyrin precursors. However, during the second challenge, the protection was maintained only in animals treated with ApoAI-PBGD mRNA (as estimated by pain score and urinary ALA and PBG excretion) (fig. S3, B to F). These data confirm that ApoAI-PBGD is more stable in the liver than the unconjugated protein.

We then performed a kinetic study analyzing hepatic PBGD activity in parallel with liquid chromatography–tandem mass spectrometry (LC-MS/MS) determination of intrahepatic content of human PBGD peptide. The study was performed in female AIP mice intravenously injected with rhPBGD, rhApoAI-PBGD, or the conjugated form of a PBGD variant (rApoAI-PBGD-I291M/N340S or PBGDms) (300 nmol/kg) containing two amino acid substitutions (I129M and N340S), which confer enhanced enzymatic activity to the protein (*15*). Animals were euthanized at different time points (4 hours and days 1, 3, 5, and 35), and PBGD activity was determined in fresh liver extracts, allocating part of the liver sample to LC-MS/MS analysis. After administering rhApoAI-PBGD or rApoAI-PBGDms, both hepatic PBGD activity and human PBGD peptide content peaked at 4 hours with progressive decay during the following days (Fig. 2, A and B). In animals given rApoAI-PBGDms, the human PBGD peptide was detectable at day 35 after treatment in conjunction with a PBGD activity still higher than that found in noninjected AIP mice. In sharp contrast, treatment with rhPBGD resulted in a very slight rise of intrahepatic human PBGD peptide and failure to increase enzymatic activity above values observed in untreated AIP mice. These results establish a clear link between hepatic PBGD activity and liver uptake of the fusion proteins. Furthermore, they also demonstrate that rApoAI-PBGDms remains functional in the liver for a sustained period of time.

To further ascertain that PBGD linked to ApoAI is internalized by liver cells, AIP mice were treated with an intravenous injection of murine apoAI-pbgd (mapoAI-pbgd) or rApoAI-PBGDms (300 nmol/kg), and 3 days later, the presence of PBGD in hepatocytes isolated from the liver of these mice was analyzed by immunofluorescence. Using confocal microscopy, we found clear PBGD reactivity in the cytoplasm of hepatocytes from mice treated with the conjugated proteins, whereas a very faint signal (likely corresponding to endogenous PBGD) was observed in untreated controls (fig. S4; green area: 0.05, 0.6, and 2.53% in A′, B′, and C′, respectively).

To gain insight into the uptake of ApoAI conjugates of PBGD into parenchymal liver cells, cultured primary mouse hepatocytes were incubated for 4 hours in the presence of rhPBGD, rPBGDms, rhApoAI-PBGD, and rApoAI-PBGDms. Then, the cells were analyzed by immunofluorescence using anti-human PBGD and confocal microscopy. We observed that both rhPBGD and rPBGDms remained localized extracellularly, whereas rhApoAI-PBGD and rApoAI-PBGDms were found within the cytoplasm (Fig. 2C). Next, we examined the role of the HDL endocytosis pathway in the transport of the conjugated proteins into liver cells. Isolated hepatocytes were incubated with rhApoAI-PBGD or rApoAI-PBGDms in the presence or absence of HDL (as a competitor) or BLT-1 (an inhibitor of SR-B1, the main HDL receptor). The immunopositive pattern was different depending on the condition used (Fig. 2D). These images suggest that the recombinant conjugated proteins showed differential access to the perinuclear region under conditions of ApoAI interaction with the HDL receptor (Fig. 2D).

To further examine the traffic of rhApoAI-PBGD into liver cells in vivo, we intravenously injected this protein (60 nmol/kg) into AIP mice with or without concomitant administration of liposomes containing chloroquine (LipoCQ), an endosomal disrupting agent (*16*). We observed that, 24 hours after protein infusion, hepatic PBGD activity increased when LipoCQ was given in conjunction with rhApoAI-PBGD (fig. S5), supporting the idea that the conjugated protein trafficked through the endocytic compartment of liver cells.

As HDL crosses the brain-blood barrier (BBB) (*17*) and acts as a carrier for rhApoAI-PBGD, we tested whether this molecule gains access to the central nervous system. In AIP mice treated intravenously with rhPBGD or rApoAI-PBGDms (60 nmol/kg) or saline, we found that only the conjugated protein was able to raise PBGD activity in cerebral tissue (fig. S6A). To get insight into the mechanism by which conjugated PBGD is transported to the brain, we analyzed the kinetics of serum and brain PBGD activity in AIP mice whose liver had been transfected with a plasmid encoding rhApoAI-PBGD linked to a signal peptide to promote its secretion. Liver transduction was performed by hydrodynamic injection, which enables transient expression of the transgenic protein. We observed that serum PBGD activity peaked at day 2 and then decreased,

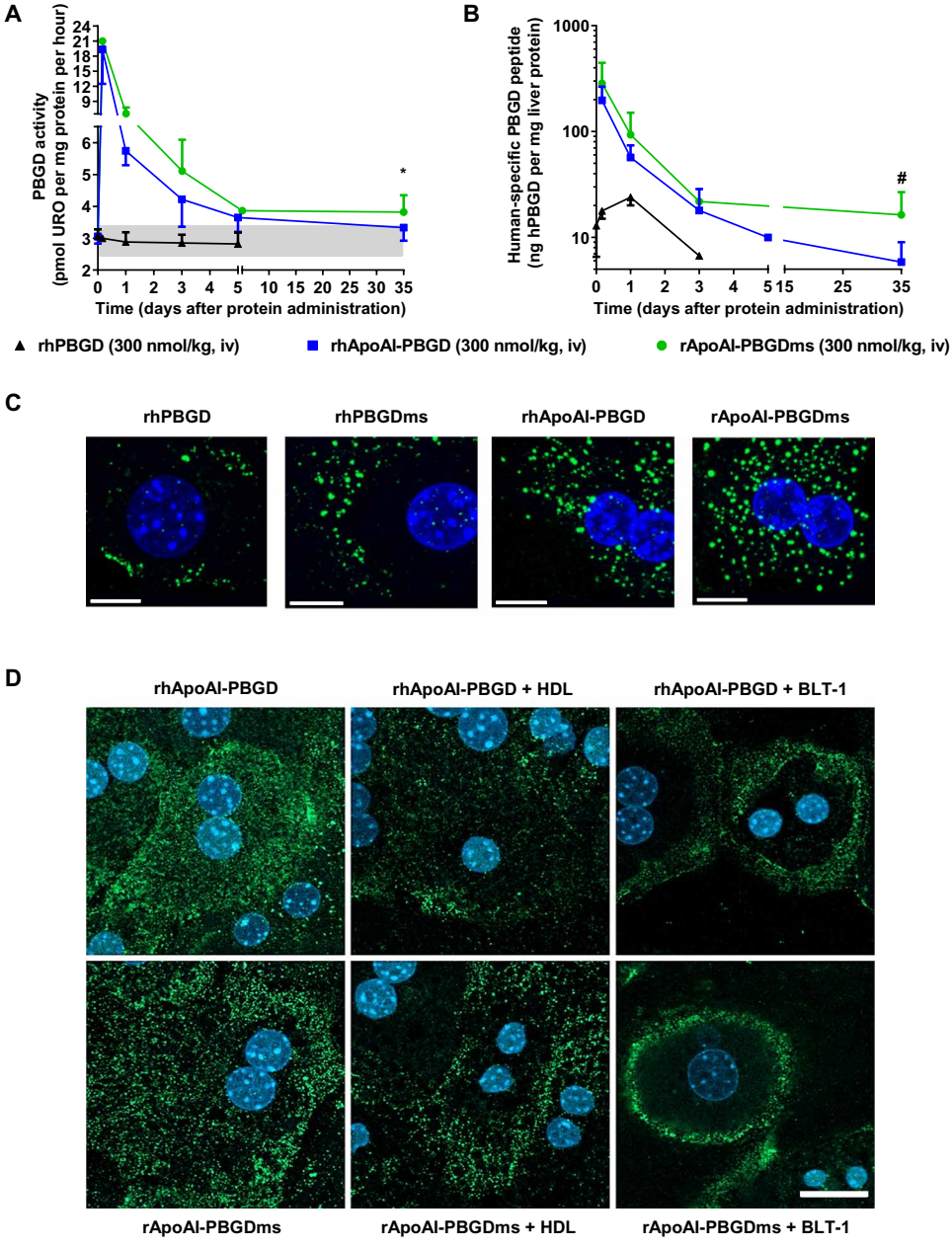

Fig. 2. ApoAI-conjugated proteins are internalized in hepatocytes. (**A**) PBGD activity and (**B**) kinetic analysis of human PBGD peptide measured by LC-MS/MS in livers from female AIP mice intravenously injected with rhApoAI-PBGD or rApoAI-PBGDms (300 nmol/kg) and euthanized at different time points (4 and 24 hours, and at days 3, 5, and 35). *$P < 0.05$ versus saline group; #$P < 0.05$ versus rhApoAI-PBGD group, two-tailed Student's t test. (**C**) Primary hepatocytes from AIP mice immunostained for PBGD (green) 4 hours after administration of unconjugated or ApoAI-conjugated proteins (PBGD and rPBGDms). Confocal microscopy pictures were taken after 4′,6-diamidino-2-phenylindole (DAPI) nuclear staining (Blue). Scale bars, 5 μm. (**D**) Confocal microscopy pictures of primary hepatocytes pretreated with HDL (100 μg/ml) or BLT-1 (30 μM) before the administration of ApoAI-conjugated proteins (rhApoAI-PBGD and rApoAI-PBGDms). Hepatocytes were immunostained for PBGD (green), and the nucleus was stained with DAPI (blue). Scale bar, 20 μm.

whereas the enzymatic activity in the brain increased progressively from days 2 to 7 after injection (fig. S6B), suggesting a saturable transport mechanism. In line with this idea, we found that, 7 days after therapy, brain PBGD activity was similar in animals that received a single dose of rhApoAI-PBGD (15, 30, or 60 nmol/kg) (fig. S6C). It should be noted that the brain vasculature was thoroughly washed before tissue processing, thus excluding circulating proteins as a source of brain PBGD activity.

Treatment of AIP mice with rhApoAI-PBGD counteracts the induction of acute porphyric attacks in a dose-dependent manner

We then proceeded to study whether the administration of rhApoAI-PBGD could abrogate acute porphyric attacks in AIP mice. Acute attacks are characterized by high urinary ALA and PBG excretion in association with pain and motor disturbance. In AIP mice, these crises were induced by administering phenobarbital for four consecutive days (Fig. 3, A to C). We found that the injection (intravenous) of a single dose of unconjugated rhPBGD (300 nmol/kg, equivalent to 12.5 mg/kg) 24 hours after the first phenobarbital dose (day 1) resulted in a very modest reduction in the rise of porphyrin precursors when compared to untreated AIP mice (Fig. 3A and fig. S7). In contrast, a single dose of rhApoAI-PBGD (30, 60, or 300 nmol/kg) (intravenous) efficiently blocked the increase of urinary ALA and PBG, an effect that was more pronounced with the higher doses. rhApoAI-PBGD was more effective at reducing heme precursors than three consecutive doses of hemin (12.27 pmol/kg per dose, equivalent to 8 mg/kg, intraperitoneally), which is the current standard treatment for acute porphyric attacks (Fig. 3A and fig. S7).

Four hours after the last phenobarbital dose (day 4), motor dysfunction and pain were assessed in AIP mice by means of the rotarod test and the mouse grimace scale, respectively (Fig. 3, B and C). Both hemin and rhApoAI-PBGD, but not rhPBGD, conferred protection against motor dysfunction. Pain was significantly ($P < 0.001$) attenuated in mice that received hemin or rhApoAI-PBGD (60 and 300 nmol/kg) but not in the other groups. Of interest, hemin administration, although less efficient at decreasing the accumulation of porphyrin precursors, highly reduced pain score when compared with AIP mice receiving recombinant protein (30 nmol/kg) (Fig. 3C). These data suggest that low heme stores and not only the increase of neurotoxic precursors might play a role in the genesis of pain.

Therapeutic efficacy was further assessed in AIP mice by administering the recombinant protein during an ongoing porphyric attack,

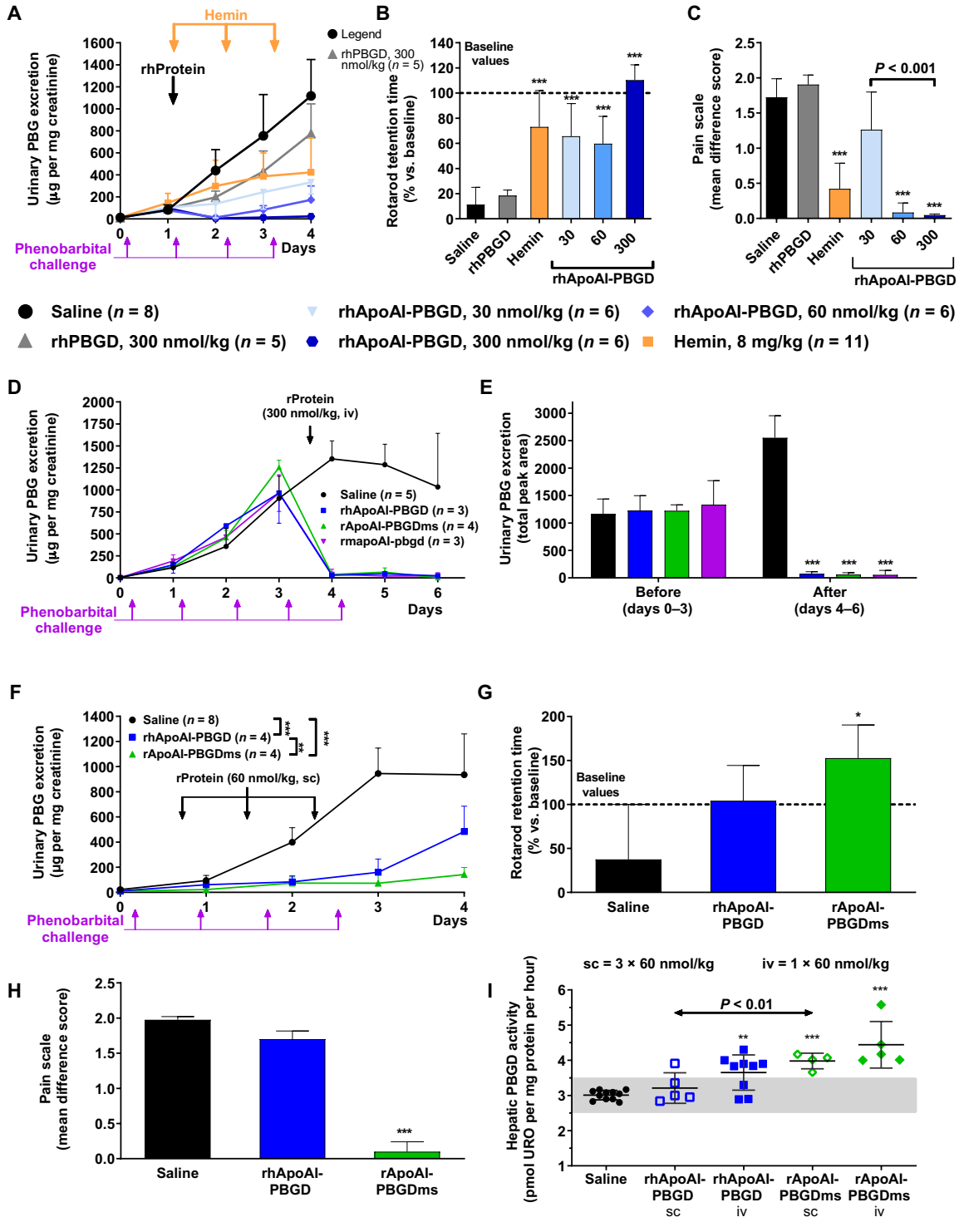

Fig. 3. rhApoAI-PBGD protects AIP mice against phenobarbital-induced acute attack. (**A**) PBG urinary excretion over four consecutive days. (**B**) Motor coordination using the rotarod test and (**C**) pain scores evaluated 4 hours after the last phenobarbital dose. (**D** and **E**) Urinary PBG excretion and quantification of total peak area before and after the administration of rhApoAI-PBGD (300 nmol/kg; $n = 5$), rApoAI-PBGDms ($n = 4$), or rmapoAI-pbgd ($n = 3$) in male AIP mice during an ongoing acute attack. (**F** to **I**) Effect of three consecutive subcutaneous (sc) doses (60 nmol/kg) of rhApoAI-PBGD or rApoAI-PBGDms in AIP mice experiencing phenobarbital-induced acute attacks ($n = 4$). (F) PBG urinary excretion over four consecutive days. Four hours after the last phenobarbital challenge, (G) motor coordination and (H) pain score were determined. (I) Hepatic PBGD activity analyzed 2 days after the last phenobarbital dose. Data are means of two independent experiments. *$P < 0.05$, **$P < 0.01$, and ***$P < 0.001$ versus control saline AIP group.

which was induced by challenging the mice with five consecutive doses of phenobarbital. Administration of a single injection of 300 nmol/kg (intravenous) of either rhApoAI-PBGD, rApoAI-PBGDms, or recombinant murine apoAI-pbgd (rmapoAI-pbgd), 2 hours after the fourth injection of phenobarbital, decreased urinary PBG excretion to baseline in only 1 day (Fig. 3, D and E). The decline in urinary ALA accumulation was slower and it reverted to normal values at day 3 post-injection (fig. S8). Thus, the three recombinant proteins were equally effective in reverting an ongoing acute attack.

Repeated subcutaneous administration of rApoAI-PBGDms counteracts recurrent acute attacks in AIP mice

The subcutaneous route of administration of a therapy would be advantageous for those patients with recurrent porphyric attacks, as it would enable self-administration of the treatment without the need for repetitive hospitalizations. Thus, we tested whether ApoAI-PBGD conjugates given subcutaneously could protect against phenobarbital-induced attacks. AIP mice were subjected to phenobarbital challenge for 4 days and treated with 3 daily subcutaneous doses of either rhApoAI-PBGD or rApoAI-PBGDms (45, 30 and 30 nmol/kg). At this dose, the treatment failed to show any substantial reduction in urinary ALA or PBG excretion (fig. S9). The following week the same mice were similarly challenged with phenobarbital but received 3 daily subcutaneous injections of rhApoAI-PBGD or rApoAI-PBGDms (60 nmol/kg). At this dose, rhApoAI-PBGD exerted a partial protective effect (Fig. 3, F to H), but rApoAI-PBGDms efficiently reduced the accumulation of both ALA and PBG and abrogated pain and motor dysfunction (fig. S9). At the end of the study (24 hours after the last dose of the therapeutic protein), hepatic PBGD activity in mice treated with subcutaneous rApoAI-PBGDms was higher than in those treated with subcutaneous rhApoAI-PBGD. Furthermore, the hepatic PBGD activity in mice treated with three daily subcutaneous injections of rApoAI-PBGDms was comparable to that observed 24 hours after a single intravenous dose (60 nmol/kg) of rhApoAI-PBGD or rApoAI-PBGDms (Fig. 3I). These findings emphasize the higher potency of rApoAI-PBGDms and also show that, despite six repeated doses of the conjugated proteins, the therapeutic efficacy is maintained, suggesting low immunogenicity of the molecules.

To gain further insight into the immunogenicity of PBGD bound to ApoAI, AIP mice were injected with four doses of mapoAI-pbgd protein (60 nmol/kg) on days 1, 7, 14, and 21. Another group of mice was administered with seven intravenous doses of rhApoAI-PBGD protein, from 1 to 6 weeks, and on week 8. Antibodies against PBGD and ApoAI were determined at different time points (fig. S10). We found that none of the five mice injected with the murine protein developed antidrug antibodies against either PBGD or ApoAI proteins. Only one of five animals injected with the human recombinant protein developed antibodies, albeit at very low titers.

A loading dose of rApoAI-PBGDms provides long-term protection against recurrent porphyric attacks in AIP mice

As mentioned, high hepatic PBGD activity was induced in AIP mice after intravenous administration of rhApoAI-PBGD (300 nmol/kg) (5.8 ± 0.5 U). When using the same dose of rApoAI-PBGDms, the enzymatic activity in the liver was raised to even higher values (7.9 ± 3.3 U, $P < 0.01$), whereas it did not change (as compared to untreated mice) after administration of rPBGDms (2.8 ± 0.3 U). We next investigated whether a single loading dose of these compounds could afford long-lasting protection against acute attacks in AIP mice. Animals were subjected to four phenobarbital challenges (four daily phenobarbital doses each challenge) over a period of 5 weeks and received a single intravenous dose of rPBGDms, rApoAI-PBGDms, or rhApoAI-PBGD (300 nmol/kg) on day 1 of the first phenobarbital challenge. To compare the protective effect of these proteins with hemin, a group of AIP mice received one intravenous dose of hemin (8 mg/kg) on days −7, −5, and −3 and on the first day of each phenobarbital challenge. Our results showed that neither rPBGDms nor hemin administration prevented the increase of urinary PBG (Fig. 4A and fig. S11A) and ALA (fig. S11, B and C) excretion at any time point during the study period. However, rhApoAI-PBGD was able to prevent the accumulation of porphyrin precursors during the first induced attack. rApoAI-PBGDms had more lasting and marked effects as it efficiently blocked the rise of PBG and ALA during the first porphyric attack and caused an important reduction in the urinary excretion of porphyrin precursors during the second, third, and fourth induced attacks (Fig. 4A and fig. S11, A to C).

Furthermore, both rApoAI-PBGDms and rhApoAI-PBGD protected against pain and motor disturbance (Fig. 4, B and C), with the therapeutic effects being longer-lasting with rApoAI-PBGDms. Moreover, after the fourth induced acute attack, the amplitude of the muscle action potential was decreased in untreated AIP mice and in those that received rPBGDms or hemin, whereas it was normal in animals treated with either rhApoAI-PBGD or rApoAI-PBGDms (fig. S11D). By the end of the study (day 35), the strong overexpression of *Alas1* gene that occurred in the liver of AIP mice as a result of repeated phenobarbital challenges was completely abrogated in the groups treated with rApoAI-PBGDms (Fig. 4D), reflecting normalization of hepatic heme metabolism in these animals. In mice treated with rhApoAI-PBGD, the decrease in *Alas1* mRNA did not reach statistical significance compared to untreated AIP controls. In accordance with these findings, as mentioned above (Fig. 2A), hepatic PBGD activity at day 35 still remained elevated in the rApoAI-PBGDms group compared to untreated AIP, but not in animals treated with rhApoAI-PBGD (fig. S11E). Thus, rApoAI-PBGDms outperforms rhApoAI-PBGD in providing AIP animals with long-lasting protection against porphyric attacks.

Long-term protection against recurrent porphyric attacks was also assayed after subcutaneous administration of the therapy. Preliminary data showed that two consecutive subcutaneous doses of the conjugated protein (300 nmol/kg) (given 24 hours apart) are needed to increase hepatic PBGD activity (24 hours after the last injection) to values similar to those achieved with a single intravenous dose (Fig. 4E). Using this subcutaneous dosing schedule, we found that rApoAI-PBGDms administered at the beginning of the study was able to protect against accumulation of porphyrin precursors, motor discoordination, and pain (Fig. 4, F to I, and fig. S12) during three phenobarbital challenges over a period of 2 weeks. These effects were comparable to those exerted by intravenous hemin given repeatedly three times in each attack. At the end of the study, mice were sacrificed to determine hepatic *Alas1* mRNA expression. We found that *Alas1* was highly induced in control AIP mice that received saline but showed normal values in porphyric animals treated with hemin or rApoAI-PBGDms (Fig. 4J).

DISCUSSION

Here, we describe a method enabling a recombinant enzyme to enter hepatocytes where it remains active for about 1 month after its

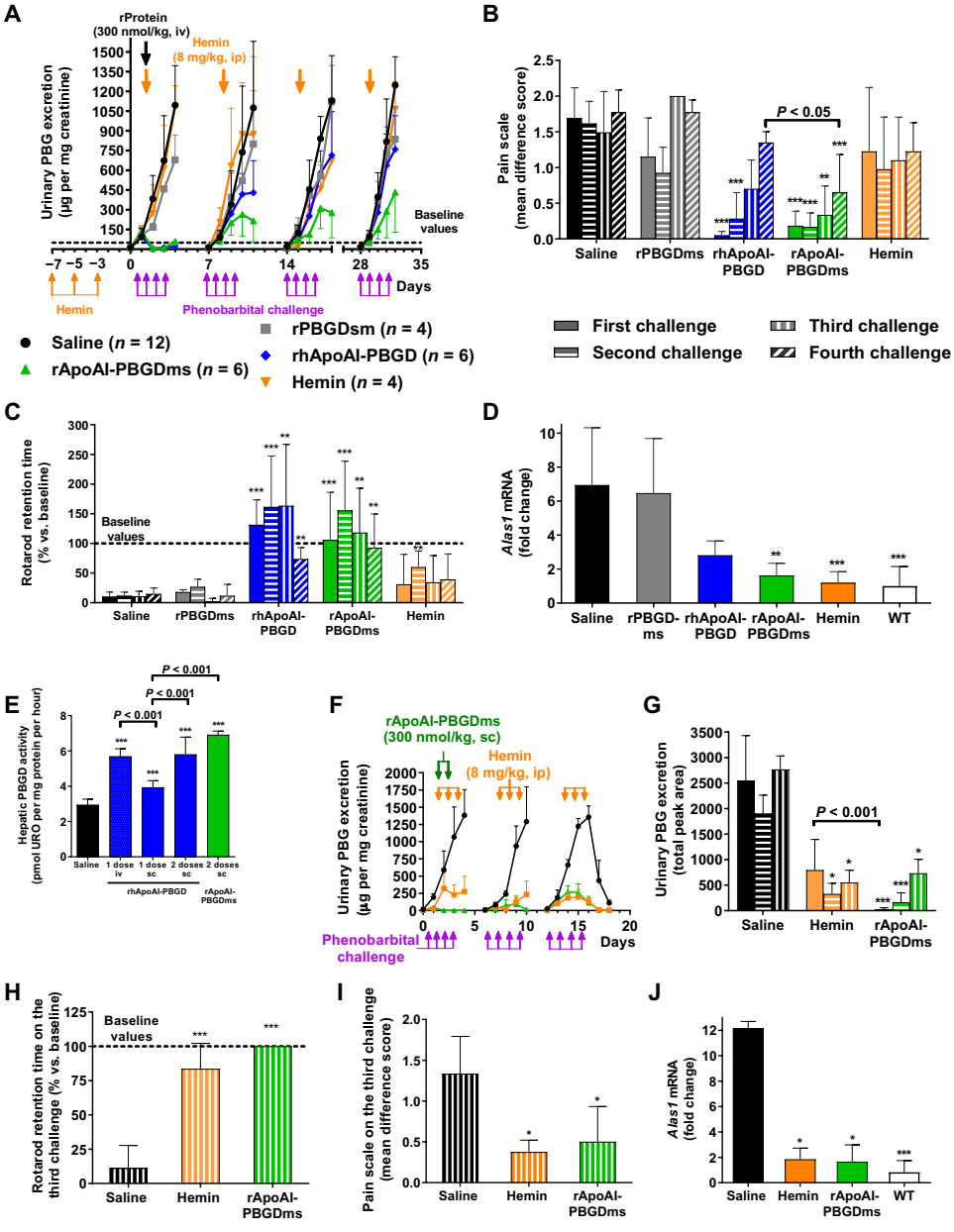

Fig. 4. Long-term protection of AIP mice against acute attacks by administration of rApoAI-PBGDms. (**A**) Twenty-four–hour urinary PBG excretion was determined in each phenobarbital challenge. ip, intraperitoneally. (**B**) Pain score and (**C**) motor coordination evaluated 4 hours after the last phenobarbital injection in each challenge. (**D**) *Alas1* expression and at sacrifice on day 35 in liver samples from all animals. (**E**) Hepatic PBGD activity after administration of one or two doses of rhApoAI-PBGD or rApoAI-PBGDms in AIP mice. (**F**) Urinary PBG excretion and (**G**) quantification of total area under the curve in AIP mice subjected to three subsequent phenobarbital challenges. (**H**) Motor coordination and (**I**) pain score determined after the fourth phenobarbital dose of the last challenge. (**J**) Hepatic *Alas1* expression at sacrifice at day 18. WT, wild type. *$P < 0.05$, **$P < 0.01$, and ***$P < 0.001$ versus saline AIP group. *$P < 0.05$, **$P < 0.01$, and ***$P < 0.001$ versus control saline in each challenge.

systemic administration. We have applied this method to treat a murine model of AIP, a PBGD deficiency causing a blockade of the heme biosynthesis pathway.

Previous reports have used peptide moieties like the transactivator of transcription (TAT) human immunodeficiency virus (HIV-Tat) peptide or fragments of the human hepatocyte growth factor (HGF) to deliver proteins, including enzyme cargo, to the liver (*18*–*21*). However, these approaches have limitations that restrict their clinical application. In particular, the HIV-Tat peptide is immunogenic and cannot be repeatedly administered, and the HGF moiety was able to maintain enzymatic activity (phenylalanine hydrolase) in mouse liver for only 6 hours, which greatly reduces its clinical utility. In this work, we show that the protein formed by linking ApoAI to the N terminus of PBGD has long half-life in circulation where it is found incorporated into HDL. After intravenous injection, rhApoAI-PBGD and the hyperfunctional rApoAI-PBGDms enter hepatocytes to enhance enzymatic function in the liver. We were able to show that, 35 days after a single loading dose of rApoAI-PBGDms, the protein was still detectable in the liver, and hepatic PBGD activity remained above that found in AIP mice. Both rhApoAI-PBGD and rApoAI-PBGDms dosed intravenously prevented and abrogated phenobarbital-induced porphyric attacks in AIP mice, with the effect of the latter protein being more durable. Intravenous administration of a single loading dose of rApoAI-PBGDms provided long-lasting protection against porphyric attacks, offering the possibility of using this therapy prophylactically in patients with very frequent attacks. Moreover, the therapeutic effect of rApoAI-PBGDms was observed not only after intravenous injection of the protein but also after its subcutaneous administration, a property that may allow patients to treat themselves when symptoms start, thereby potentially avoiding hospitalization.

Previous findings from our group, and from other authors, have shown that only a small increase of PBGD hepatic activity above the values present in AIP animals is enough to protect against porphyria crises (*10*, *22*–*24*). As indicated before, the administration of PBGD bound to ApoAI leads to an enhancement of hepatic PBGD activity that resolves and prevents porphyric attacks. Unlike hemin or givosiran, the two approved therapies for AIP (*3*, *25*), which act through repression of *Alas1* induction (by increasing heme stores or via RNA interference, respectively), rhApoAI-PBGD or rApoAI-PBGDms, restores hepatic PBGD activity and the regulation of the heme synthesis pathway.

Our results show that, after systemic administration, rhApoAI-PBGD and rApoAI-PBGDms penetrate liver cells, where they seemingly undergo endosomal trafficking, as has been described for endogenous ApoAI (*26*). The observation that liposomal chloroquine

given concurrently with rhApoAI-PBGD enhances hepatic PBGD activity is consistent with this concept. Because PBGD functions in the cytosol, the administered protein would have to exit the endosomes to fulfill its function. The mechanism by which this would occur has not been clarified, but might be related to increased endosomal cargo after the injection of sufficiently high doses of the ApoAI conjugates. We observed that rhApoAI-PBGD is preferentially taken up by zone 3 hepatocytes. This is an interesting finding, as genes of the heme synthesis pathway are more abundantly expressed in this area (*27*).

The injection of PBGD bound to ApoAI increased PBGD activity not only in the liver but also in the brain. It should be noted that rhApoAI-PBGD circulates incorporated into HDLs and that transcellular transport of HDL across the BBB is an important property of these lipoproteins (*28*). Here, we present data indicating that rhApoAI-PBGD crosses the BBB via a saturable transport mechanism, as our group has previously reported for other proteins linked to ApoAI (*29*). Brain PBGD activity was measured after thoroughly washing cerebral vessels, thus excluding intravascular protein as a source of enzymatic activity. In our study, we were unable to obtain conclusive information on the cerebral distribution of the recombinant proteins. Unfortunately, the sensitivity of the immunohistochemical method did not allow us to establish the cell type (vascular endothelium, neurons, and glia) where the exogenous PBGD was located. However, irrespective of the cell type, the penetration of PBGD into the brain may contribute to the local elimination of toxic porphyrin precursors within the cerebral tissue during porphyric attacks. Further studies are needed to define the type of cell in the central nervous system where the fusion ApoAI proteins localize after their intravenous or subcutaneous administration.

In common with other enzyme replacement therapies using recombinant proteins, a potential limitation of our therapeutic approach is that repeated administration of the fusion protein might induce neutralizing antibodies. However, in a previous clinical trial in patients with AIP treated with intravenous rhPBGD, no substantial neutralizing antibodies against the recombinant protein and no adverse effects were observed. Only 7 of 40 subjects involved in the trial developed non-neutralizing antibodies against rhPBGD (*11*). In our AIP mice, the therapeutic efficacy is maintained after the administration of six repeated doses of rhApoAI-PBGD or rApoAI-PBGDms. Moreover, in AIP mice receiving four weekly doses of murine or human ApoAI PBGD conjugates, none of those given the murine protein developed antibodies, and only one of the five animals injected with the human protein generated low antibody titers. Although our findings indicate low immunogenicity of ApoAI-PBGD conjugates, the potential development of neutralizing antibodies upon long-term iterative administration of the therapy should be carefully monitored in future clinical trials. Another limitation for translating the recombinant conjugated ApoAI proteins to the clinical arena might emerge with large-scale production; thus, further optimization of the process should be carefully considered.

In conclusion, we describe a system enabling a functional enzyme to enter parenchymal liver cells after its intravenous or subcutaneous injection, and we show that this treatment modality can be used to correct hepatic enzymatic defects like AIP in a preclinical model.

MATERIALS AND METHODS

Study design

To evaluate the therapeutic efficacy of rPBGD proteins conjugated to ApoAI, we designed pharmacokinetic studies with the recombinant ApoAI-conjugated proteins after intravenous or subcutaneous administration in female AIP mice (10 to 20 weeks old). We determined serum and hepatic PBGD activity, as well as the presence of PBGD protein by immunoblot and immunohistochemistry (IHC), and a PBGD peptide by LC-MS/MS in liver samples at different time points. Next, we designed in vitro studies to gain insight into the uptake of ApoAI conjugates of PBGD into primary mouse hepatocytes by immunofluorescence analysis and confocal microscopy. For pharmacodynamic studies, male AIP mice (10 to 16 weeks old) challenged with phenobarbital were intravenously or subcutaneously injected with rhPBGD, rhApoAI-PBGD, rApoAI-PBGDms, and rmApoAI-PBGD to compare their short- and long-term efficacy in preventing acute porphyria attacks. For this purpose, ALA and PBG urinary excretion and behavioral studies (pain and motor coordination tests) were assayed; besides, hepatic heme synthesis pathway status was analyzed after sacrifice (*Alas1* expression and PBGD activity). Experimental protocols were approved by the Ethics Committee of the University of Navarra (CEEA009-11 and CEEA048-15), according to European Council guidelines.

Mouse strains

Compound heterozygote mice [C57BL/6-$^{pbgdtm1(neo)Uam}$/C57BL/6-$^{pbgdtm2(neo)Uam}$] were used as a disease model for AIP (*30*). Biochemical alterations in this mouse model resemble those of human porphyria, mainly decreased hepatic PBGD activity (30% of steady-state values) and increased urinary excretion of the heme precursors PBG and ALA after treatment with drugs such as phenobarbital (*22*).

Production of recombinant proteins

rhPBGD-ApoAI (68 kDa), mapoAI-pbgd and rhApoAI-PBGD (68 kDa), rApoAI-PBGDms (68 kDa), rhPBGD (42 kDa), and rPBGDms (42 kDa) were produced and purified by GenScript (sequences are detailed in the Supplementary Materials). The complete sequence was subcloned into target Expression Vector E3 for *Escherichia coli* expression. *E. coli* BL21 (DE3) was transformed with recombinant plasmids, and a single colony was inoculated into lysogeny broth medium containing relevant antibiotic. Isopropyl-β-D-thiogalactopyranoside (IPTG) was introduced for induction of the recombinant proteins. Cells were harvested by centrifugation, and cell pellets were lysed by sonication. Target protein was isolated from supernatant after a one-step purification using a nickel column. Proteins were dialyzed, followed by 0.22-μm filter sterilization, and analyzed by SDS–polyacrylamide gel electrophoresis (PAGE) and Western blot using a mouse anti-His mAb (GenScript, catalog no. A00186). The purity of the recombinant proteins was estimated by size exclusion chromatography–multiangle light scattering and was determined to be 94.7% for rhPBGD and 98.6% for rPBGDms. The conjugated proteins showed 70% purity in the case of rhApoAI-PBGD (20% were aggregates of higher molecular mass and 10% were degradation products) and 67% in the case of rApoAI-PBGDms (19% were aggregates and 13% were degradation products). Endotoxin concentration was lower than 0.4 EU/μg (LAL Endotoxin Assay Kit; GenScript, catalog no. L00350). The concentration of the recombinant protein productions was determined by a commercial ApoAI ELISA kit (Mabtech AB, 37101HP2). The functionality of the enzyme was confirmed in vitro by determination of PBGD activity (*22*). The specific activity of the purified protein rApoAI-PBGDms is higher than that of rhApoAI-PBGD (104.4 ± 22.8 pmol uroporphyrin/mg

per hour versus 72.9 ± 13.3 pmol uroporphyrin/mg per hour, $P < 0.01$). Conjugation with ApoAI did not modify the activity of the human PBGD (78.2 ± 7.6 pmol uroporphyrin/mg per hour of rhPBGD versus rhApoAI-PBGD, not significant).

Chloroquine-encapsulated liposomes

LipoCQ was prepared by the film hydration method. Briefly, the lipids HSPC (L-α-phosphatidylcholine, hydrogenated), cholesterol, and DSPE-PEG2000 (1,2-distearoyl-sn-glycero-3-phosphoethanolamine-*N*-[methoxy(polyethyleneglycol)-2000]) at a molar ratio of 1.85:1:0.12 were dissolved in a solution of chloroform:methanol [9:1 (v/v)]. The film, formed by evaporation of the organic solvents at 65°C (Büchi), was hydrated with a buffer solution of ammonium sulfate (250 mM) at pH 5.5 (Büchi Waterbath, B-480). Liposomes, extruded through a polycarbonate membrane (100 nm pore) using a Mini-Extruder device (Avanti Polar Lipids Inc.), were washed for 1 hour at 4°C in Hepes saline buffer at pH 7.4 using the Amicon system (10,000 molecular weight cutoff) (EMD Millipore). This formulation was incubated at 60°C with chloroquine at a molar ratio of 1:0.15 in a thermoshaker for 1 hour. Formulated chloroquine liposomes were washed in Hepes saline buffer at pH 6.7 and characterized. Particle size (about 130 ± 1.2 nm) was analyzed by laser diffractometry (Zetasizer Nano Series, Malvern Instruments Limited) and showed a homogeneous population of liposomes with high encapsulation efficiency (about 97%) that was measured by spectrophotometry at 343 nm (*31*).

Production of lipid nanoparticles containing modified mRNAs encoding the human PBGD or ApoAI-PBGD protein

As previously described (*10*), the mRNAs were synthesized in vitro by T7 RNA polymerase–mediated transcription from a linearized DNA template, which incorporates the 5′ and 3′ untranslated regions and a poly-A tail. The mRNAs used Cap1 and full replacement of uridine with N1-methylpseudouridine to increase mRNA potency. After purification, the mRNA was diluted in acetate buffer to the desired concentration and formulated for intravenous delivery using a procedure previously described (*10*).

Pharmacokinetic studies

The serum half-life of the recombinant proteins was analyzed in female AIP mice ($n \geq 5$ per group) after intravenous administration of recombinant protein (60 nmol/kg, equivalent to 4.08 mg/kg). Blood samples were collected at different time points (5 min, 10 min, 30 min, 60 min, 2 hours, 4 hours, 8 hours, 24 hours, 48 hours, 3 days, 4 days, 5 days, 6 days, and 7 days). Samples were centrifuged for 5 min at 2.3*g*, and PBGD activity was biochemically determined using 15 μl of fresh plasma as previously described (*22*). Half-life was calculated using the Prism 6.0 computer program (GraphPad Software), fitting the one-phase decay of the PBGD activity.

Detection of the recombinant proteins in serum lipoprotein fractions

To analyze whether unconjugated and conjugated rhPBGD protein circulates bound to lipoproteins, recombinant proteins (60 nmol/kg) were injected intravenously via tail vein injection. Blood samples were collected in AIP mice at 36 hours after injection for rhPBGD and 72 hours for rhApoAI-PBGD, and different lipoprotein fractions were extracted from the serum. Briefly, 400 μl of serum was mixed with 1100 μl of sodium bromide (NaBr, Fluka, Merck) buffer at a density (ρ) of 1.006 g/liter. Samples were centrifuged at 256,516*g* for 2 hours at 4°C, and serum lipoproteins were distributed on a density gradient. At the top, VLDL was collected. Then, a new NaBr buffer (ρ = 1.4 g/liter) was added, adjusting the final density to 1.04 g/liter. A second centrifugation (256,516*g*) for 2.5 hours distributes the LDL fraction to the top. Last, another centrifugation (256,516*g*) for 3 hours after the addition of NaBr buffer (ρ = 1.4 g/liter, adjusting the final density to 1.21 g/liter) was performed, which shifted the HDL fraction to the top.

The presence of conjugated rhPBGD protein in each of the fractions was determined by enzymatic activity (*22*) and by Western blot analysis. Briefly, 15 μl of each lipoprotein fraction was mixed 1:3 with sample buffer [containing 50% glycerol, 10% SDS, 300 mM tris (pH 6.8), and 0.05% bromophenol blue] and heated for 5 min at 95°C. For each sample, proteins were separated by 8% SDS-PAGE and transferred to a nitrocellulose membrane (Whatman). The membrane was blocked (5% milk in tris-buffered saline–Tween 20 (0.1% TBS-T)] for 1 hour at room temperature and washed three times. Recombinant protein was detected using a rabbit polyclonal antibody against PBGD diluted 1:200 (H-300, Santa Cruz Biotechnology) or with a goat polyclonal antibody against ApoAI diluted 1:400 (E-20, Santa Cruz Biotechnology) overnight at 4°C. Horseradish peroxidase (HRP)–labeled secondary antibodies against rabbit (Sigma-Aldrich) or goat (R&D Systems) immunoglobulin G (IgG), respectively, were diluted 1:10,000; the membrane was then washed again with 0.1% TBS-T; and the proteins were detected using a Western Lightning Plus ECL kit (PerkinElmer) according to the manufacturer's instructions. Prestained protein standards with a molecular mass range from 205 to 7 kDa were used (Bio-Rad).

Western blot, liver IHC, and hepatic PBGD activity

Female AIP mice received a single intravenous administration (30, 60, or 300 nmol/kg, equivalent to 2.04, 4.08, or 20.4 mg/kg, respectively) or three consecutive subcutaneous doses of recombinant conjugated proteins (60 nmol/kg) ($n \geq 5$ per group). As a control, female AIP mice groups received unconjugated PBGD (300 nmol/kg, $n = 4$) or saline ($n = 8$). At sacrifice, mice were perfused with prewarmed phosphate-buffered saline to eliminate the blood from the liver. For Western blot assay, liver samples were homogenized in radioimmunoprecipitation assay (RIPA) lysis buffer [50 mM tris-HCl (pH 7.4), 150 mM KCl, 0.1% SDS, 2% NP-40, 10 mM sodium deoxycholate, and Protease Inhibitor Cocktail cOmplete 1X (Roche Diagnostics S.L.)] and protein concentrations were determined using the Bio-Rad Protein Assay Dye Reagent Concentrate Kit. Each sample (30 to 50 μg) was resolved by 12% acrylamide gel for SDS-PAGE and transferred to a polyvinylidene difluoride or nitrocellulose membrane. Membranes were blocked with 5% milk in TBS containing 0.1% Tween 20 for 1 hour at room temperature and incubated overnight at 4°C with the specific antibody: anti-PBGD antibody (1:1000 dilution; Abcam, ab129092), anti-ApoAI (1:500 dilution; Santa Cruz Biotechnology, sc-30089), and anti-GAPDH antibody (1:10,000 dilution; Cell Signaling Technology Inc., ref. 2118). Then, blots were probed with HRP-conjugated anti-rabbit IgG antibody (1:10,000 dilution; Cell Signaling Technology Inc., ref. 7074). Signals were detected using a Western Lightning Plus ECL kit (PerkinElmer). IHC to detect PBGD in hepatic tissue was performed in formalin-fixed liver sections using a human PBGD antibody (Novus Biologicals, NBP2-33600) as previously described (*10*). PBGD enzyme activity was determined in fresh liver extracts as previously

reported (*22*). The exogenous PBGD expression was also monitored in the liver by LC-MS/MS measurements. Mouse livers were homogenized in a buffer containing 100 mM ammonium bicarbonate and 8 M urea. Each sample was spiked with isotopically labeled signature peptide specific for human PBGD (ASYPGLQFEIIAMSTTGDK, natural C and N atoms on lysine are fully replaced by 13C and 15N isotopes, respectively; Thermo Pierce) as an internal standard. Measurements were performed in the Thermo Easy 1000 nano-UPLC, Orbitrap Fusion Mass Spectrometer, as previously described (*32*).

Brain PBGD activity

Transcardial perfusion with saline was performed at sacrifice to remove all blood from the brain. PBGD activity was determined in fresh brain homogenates by the conversion ratio of PBG to uroporphyrin per hour, as previously described for liver samples (*22*). To assess whether rhApoAI-PBGD was delivered to neurons or glia, circulating into brain capillary or only incorporated in its endothelial cell, an IHC with an anti-PBGD antibody was performed on frozen brain samples.

Confocal microscopy

A total of 200,000 primary hepatocytes from male AIP mice were seeded in glass coverslips previously covered with collagen (Menzel-Glaser) in 12-well plates and starved for 4 hours before addition of the recombinant proteins rhApoAI-PBGD, rApoAI-PBGDms, rhPBGD, or rPBGDms (200 μM). Cells treated with phosphate-buffered saline were also analyzed as a negative control, and all conditions were performed in duplicate. Four hours after the treatment, cells were fixed with formaldehyde, washed three times, blocked with 2% bovine serum albumin and 3% normal goat serum, and incubated with the PBGD antibody (1:800 in blocking solution) overnight at 4°C. The secondary antibody used for detection was an Alexa Fluor 488–conjugated goat anti-rabbit IgG (1:400 dilution, 1 hour at room temperature; Abcam, ab150077). Then, cells were washed and mounted in mounting medium with 4′,6-diamidino-2-phenylindole (DAPI). Cells were viewed on an LSM 800 confocal microscope (Carl Zeiss Microscopy S.L.). Pictures were taken with an AxioCam HR digital camera, and images were acquired with the LSM acquisition software (Carl Zeiss Microscopy S.L.).

Induction of acute porphyric attacks in AIP mice and therapeutic effect of rhApoAI-PBGD or rApoAI-PBGDms proteins

Pharmacodynamic studies were performed with male mice because they have increased sensitivity to phenobarbital as evidenced by a greater induction of hepatic ALAS1 and accumulation of precursors after the phenobarbital challenge, as previously reported (*33*). The therapeutic effect of rhApoAI-PBGD and rhApoAI-PBGD was tested in male AIP mice in which acute porphyric attacks were induced by intraperitoneal administration of four increasing doses of phenobarbital at 24-hour intervals (75, 80, 85, and 90 mg/kg body weight). After each phenobarbital dose, mice were housed in metabolic cages to collect 24-hour urine samples. For porphyrin precursor measurements, PBG was retained in buffer anion-exchange resin (BioSystems SA) and eluted with acetic acid (1 M), and the Ehrlich's reaction product was spectrophotometrically quantified at 555 nm in Ultrospec 3000 (Amersham Pharmacia Biotech). ALA was retained in buffer cation-exchange resin (BioSystems SA) and eluted with sodium acetate (1 M). The eluate was incubated in a boiling water bath for 10 min in the presence of acetylacetone to form PBG and then measured as described above. An ALA standard that followed the same cycling process allowed quantification and to normalize the amount of precursor present in each study. Last, daily urinary PBG and ALA excretion were normalized to urine creatinine values.

Pain assessment, rotarod test (Ugo Basile 7650), and gait analysis (*10*) were performed in mice 4 to 6 hours after the last phenobarbital injection of each induced acute attack. Facial expression [orbital tightening, nose bulge, cheek bulge, ear position, and whisker change (*34*)] and other parameters such as abdominal grooming, motor coordination, and respiratory distress were scored to quantify the subjective experience of pain after each of the challenges. Neuromotor impairment was measured analyzing the retention time on a rotarod. Baseline retention time was 100% for each mouse, and results obtained after the phenobarbital-induced acute attacks were plotted as a percentage of basal retention time ± SD. Action potential amplitude of the sciatic nerve was measured for the long-term efficacy study after four recurrent acute attacks on day 32, 8 hours after the last phenobarbital dose.

RNA extraction and quantitative polymerase chain reaction (qPCR) determination of hepatic expression of Alas1 were performed as reported (*4*). Briefly, mRNA was extracted from liver tissues using TRIzol (Invitrogen, Thermo Fisher Scientific Inc.) and then converted into complementary DNA (cDNA) by reverse transcription PCR (RT-PCR). qPCR was performed using specific primers annealing [forward primer, 5′-CAAAGAAACCCCTCCAGCCAATGA-3′; reverse primer, 5′- GCTGTGTGCCGTCTGGAGTCTGTG-3′; product length, 101 base pairs (bp)] and iQ SYBR Green Supermix in an iQ5 real-time PCR detection system (Bio-Rad). The relative amount of gene transcripts was calculated as the *n*-fold difference compared to the control mouse β-actin gene as an internal control (forward primer, 5′-CGCGTCCACCCGCGAG-3′; reverse primer, 5′-CCTGGTGCCTAGGGCG-3′; product length, 193 bp). Results are expressed according to the formula $2\Delta^{Ct(Actin) - \Delta Ct(gene)}$, where ΔCt represents the difference in threshold cycle between the target and control genes.

Anti-drug antibody enzyme-linked immunosorbent assay

In a multiwell plate (conical bottom plates) coated with antigen, 2.5 μl of blood serum diluted 1:20 with assay diluent was deposited in wells A and B. Then, samples were successively diluted 1:2 with assay diluent from wells B to H. After adding the Protein A-HRP (0.5 mg; Sigma-Aldrich, ref. P8651) in blocking solution with a 1:5000 dilution, and the enzyme substrate (TMB Substrate Reagent; BD Biosciences, ref. 555214), absorbance was read at 450 nm. Serum samples taken before protein administration were used as negative control, and a commercial anti-PBGD antibody (Abcam, ab129092) was used as positive control.

Statistical analyses

Results were plotted as means ± SD. Data were transformed using the formula $\log(1 + x)$ to normalize the variances. Student's *t* tests were used to compare two groups, and differences between more than two groups were detected using a one-way analysis of variance (ANOVA). Pairwise comparisons were made using Bonferroni's multiple comparison tests. Differences were statistically significant when $P < 0.05$. Statistical analyses were carried out with GraphPad Prism 6.0 (GraphPad Software).

SUPPLEMENTARY MATERIALS

www.science.org/doi/10.1126/scitranslmed.abc0700
Sequence of the recombinant conjugated ApoAI-PBGD proteins and supplementary Figs. S1 to S12
Data file S1

View/request a protocol for this paper from *Bio-protocol*.

REFERENCES AND NOTES

1. M. Balwani, B. Wang, K. E. Anderson, J. R. Bloomer, D. M. Bissell, H. L. Bonkovsky, J. D. Phillips, R. J. Desnick; Porphyrias Consortium of the Rare Diseases Clinical Research Network, Acute hepatic porphyrias: Recommendations for evaluation and long-term management. *Hepatology* **66**, 1314–1322 (2017).
2. L. Gouya, P. Ventura, M. Balwani, D. M. Bissell, D. C. Rees, U. Stölzel, J. D. Phillips, R. Kauppinen, J. G. Langendonk, R. J. Desnick, J.-C. Deybach, H. L. Bonkovsky, C. Parker, H. Naik, M. Badminton, P. E. Stein, E. Minder, J. Windyga, R. Bruha, M. D. Cappellini, E. Sardh, P. Harper, S. Sandberg, A. K. Aarsand, J. Andersen, F. Alegre, A. Ivanova, N. Talbi, A. Chan, W. Querbes, J. Ko, C. Penz, S. Liu, T. Lin, A. Simon, K. E. Anderson, EXPLORE: A prospective, multinational, natural history study of patients with acute hepatic porphyria with recurrent attacks. *Hepatology* **71**, 1546–1558 (2020).
3. A. Fontanellas, M. A. Ávila, K. E. Anderson, J.-C. Deybach, Current and innovative emerging therapies for porphyrias with hepatic involvement. *J. Hepatol.* **71**, 422–433 (2019).
4. C. Schmitt, H. Lenglet, A. Yu, C. Delaby, A. Benecke, T. Lefebvre, P. Letteron, V. Paradis, S. Wahlin, S. Sandberg, P. Harper, E. Sardh, A. K. Sandvik, J. R. Hov, A. K. Aarsand, L. Chiche, C. Bazille, J.-Y. Scoazec, J. To-Figueras, M. Carrascal, J. Abian, A. Mirmiran, Z. Karim, J.-C. Deybach, H. Puy, K. Peoc'h, H. Manceau, L. Gouya, Recurrent attacks of acute hepatic porphyria: Major role of the chronic inflammatory response in the liver. *J. Intern. Med.* **284**, 78–91 (2018).
5. E. Sardh, P. Harper, M. Balwani, P. Stein, D. Rees, D. M. Bissell, R. Desnick, C. Parker, J. Phillips, H. L. Bonkovsky, D. Vassiliou, C. Penz, A. Chan-Daniels, Q. He, W. Querbes, K. Fitzgerald, J. B. Kim, P. Garg, A. Vaishnaw, A. R. Simon, K. E. Anderson, Phase 1 trial of an RNA interference therapy for acute intermittent porphyria. *N. Engl. J. Med.* **380**, 549–558 (2019).
6. J. To-Figueras, R. Wijngaard, J. García-Villoria, A. K. Aarsand, P. Aguilera, R. Deulofeu, M. Brunet, À. Gómez-Gómez, O. J. Pozo, S. Sandberg, Dysregulation of homocysteine homeostasis in acute intermittent porphyria patients receiving heme arginate or givosiran. *J. Inherit. Metab. Dis.* **44**, 961–971 (2021).
7. A. Fontanellas, M. A. Ávila, E. Arranz, R. E. de Salamanca, M. Morales-Conejo, Acute intermittent porphyria, givosiran, and homocysteine. *J. Inherit. Metab. Dis.* **44**, 790–791 (2021).
8. P. E. Petrides, M. Klein, E. Schuhmann, H. Torkler, B. Molitor, C. Loehr, Z. Obermeier, M. K. Beykirch, Severe homocysteinemia in two givosiran-treated porphyria patients: Is free heme deficiency the culprit? *Ann. Hematol.* **100**, 1685–1693 (2021).
9. D. D'Avola, E. López-Franco, B. Sangro, A. Pañeda, N. Grossios, I. Gil-Farina, A. Benito, J. Twisk, M. Paz, J. Ruiz, M. Schmidt, H. Petry, P. Harper, R. E. de Salamanca, A. Fontanellas, J. Prieto, G. González-Aseguinolaza, Phase I open label liver-directed gene therapy clinical trial for acute intermittent porphyria. *J. Hepatol.* **65**, 776–783 (2016).
10. L. Jiang, P. Berraondo, D. Jericó, L. T. Guey, A. Sampedro, A. Frassetto, K. E. Benenato, K. Burke, E. Santamaría, M. Alegre, Á. Pejenaute, M. Kalariya, W. Butcher, J.-S. Park, X. Zhu, S. Sabnis, E. S. Kumarasinghe, T. Salerno, M. Kenney, C. M. Lukacs, M. A. Ávila, P. G. V. Martini, A. Fontanellas, Systemic messenger RNA as an etiological treatment for acute intermittent porphyria. *Nat. Med.* **24**, 1899–1909 (2018).
11. E. Sardh, L. Rejkjær, D. E. H. Andersson, P. Harper, Safety, pharmacokinetics and pharmocodynamics of recombinant human porphobilinogen deaminase in healthy subjects and asymptomatic carriers of the acute intermittent porphyria gene who have increased porphyrin precursor excretion. *Clin. Pharmacokinet.* **46**, 335–349 (2007).
12. M. Lissing, G. Nowak, R. Adam, V. Karam, A. Boyd, L. Gouya, W. Meersseman, E. Melum, U. Ołdakowska-Jedynak, F. P. Reiter, J. Colmenero, R. Sanchez, U. Herden, J. Langendonk, P. Ventura, H. Isoniemi, O. Boillot, F. Braun, S. Perrodin, E. Mowlem, S. Wahlin; European Liver and Intestine Transplant Association, Liver transplantation for acute intermittent porphyria. *Liver Transpl.* **27**, 491–501 (2021).
13. C. Glass, R. C. Pittman, D. B. Weinstein, D. Steinberg, Dissociation of tissue uptake of cholesterol ester from that of apoprotein A-I of rat plasma high density lipoprotein: Selective delivery of cholesterol ester to liver, adrenal, and gonad. *Proc. Natl. Acad. Sci. U.S.A.* **80**, 5435–5439 (1983).
14. S. Acton, A. Rigotti, K. T. Landschulz, S. Xu, H. H. Hobbs, M. Krieger, Identification of scavenger receptor SR-BI as a high density lipoprotein receptor. *Science* **271**, 518–520 (1996).
15. I. Serrano-Mendioroz, A. Sampedro, N. Serna, R. E. de Salamanca, A. Sanz-Parra, F. Corrales, P. Berraondo, O. Millet, A. Fontanellas, Bioengineered PBGD variant improves the therapeutic index of gene therapy vectors for acute intermittent porphyria. *Hum. Mol. Genet.* **27**, 3688–3696 (2018).
16. D. J. Sullivan Jr., I. Y. Gluzman, D. G. Russell, D. E. Goldberg, On the molecular mechanism of chloroquine's antimalarial action. *Proc. Natl. Acad. Sci. U.S.A* **93**, 11865–11870 (1996).
17. K. Y. Fung, C. Wang, S. Nyegaard, B. Heit, G. D. Fairn, W. L. Lee, SR-BI mediated transcytosis of HDL in brain microvascular endothelial cells is independent of caveolin, clathrin, and PDZK1. *Front Physiol.* **8**, 841 (2017).
18. R. Eavri, H. Lorberboum-Galski, A novel approach for enzyme replacement therapy: The use of phenylalanine hydroxylase-based fusion proteins for the treatment of phenylketonuria. *J. Biol. Chem.* **282**, 23402–23409 (2007).
19. E. Coulstock, J. Sosabowski, M. Ovečka, R. Prince, L. Goodall, C. Mudd, A. Sepp, M. Davies, J. Foster, J. Burnet, G. Dunlevy, A. Walker, Liver-targeting of interferon-alpha with tissue-specific domain antibodies. *PLOS ONE* **8**, e57263 (2013).
20. J. An, C. Harms, G. Lättig-Tünnemann, G. Sellge, A. D. Mandić, Y. Malato, A. Heuser, M. Endres, C. Trautwein, S. Donath, TAT-apoptosis repressor with caspase recruitment domain protein transduction rescues mice from fulminant liver failure. *Hepatology* **56**, 715–726 (2012).
21. S. R. Schwarze, A. Ho, A. Vocero-Akbani, S. F. Dowdy, In vivo protein transduction: Delivery of a biologically active protein into the mouse. *Science* **285**, 1569–1572 (1999).
22. C. Unzu, A. Sampedro, I. Mauleón, L. Vanrell, J. Dubrot, R. E. de Salamanca, G. González-Aseguinolaza, I. Melero, J. Prieto, A. Fontanellas, Porphobilinogen deaminase over-expression in hepatocytes, but not in erythrocytes, prevents accumulation of toxic porphyrin precursors in a mouse model of acute intermittent porphyria. *J. Hepatol.* **52**, 417–424 (2010).
23. C. Unzu, A. Sampedro, I. Mauleón, M. González-Aparicio, R. E. de Salamanca, J. Prieto, T. Aragón, A. Fontanellas, Helper-dependent adenoviral liver gene therapy protects against induced attacks and corrects protein folding stress in acute intermittent porphyria mice. *Hum. Mol. Genet.* **22**, 2929–2940 (2013).
24. M. Yasuda, D. F. Bishop, M. Fowkes, S. H. Cheng, L. Gan, R. J. Desnick, AAV8-mediated gene therapy prevents induced biochemical attacks of acute intermittent porphyria and improves neuromotor function. *Mol. Ther.* **18**, 17–22 (2010).
25. Y. Y. Syed, Givosiran: A review in acute hepatic porphyria. *Drugs* **81**, 841–848 (2021).
26. P. Zanoni, S. Velagapudi, M. Yalcinkaya, L. Rohrer, A. von Eckardstein, Endocytosis of lipoproteins. *Atherosclerosis* **275**, 273–295 (2018).
27. A. Braeuning, M. Schwarz, Zonation of heme synthesis enzymes in mouse liver and their regulation by β-catenin and Ha-ras. *Biol. Chem.* **391**, 1305–1313 (2010).
28. M. Danik, D. Champagne, C. Petit-Turcotte, U. Beffert, J. Poirier, Brain lipoprotein metabolism and its relation to neurodegenerative disease. *Crit. Rev. Neurobiol.* **13**, 357–407 (1999).
29. J. Fioravanti, J. Medina-Echeverz, N. Ardaiz, C. Gomar, Z. P. Parra-Guillén, J. Prieto, P. Berraondo, The fusion protein of IFN-α and apolipoprotein A-I crosses the blood–brain barrier by a saturable transport mechanism. *J. Immunol.* **188**, 3988–3992 (2012).
30. R. L. P. Lindberg, C. Porcher, B. Grandchamp, B. Ledermann, K. Bürki, S. Brandner, A. Aguzzi, U. A. Meyer, Porphobilinogen deaminase deficiency in mice causes a neuropathy resembling that of human hepatic porphyria. *Nat. Genet.* **12**, 195–199 (1996).
31. L. Li, T. L. M. ten Hagen, M. Hossann, R. Süss, G. C. van Rhoon, A. M. M. Eggermont, D. Haemmerich, G. A. Koning, Mild hyperthermia triggered doxorubicin release from optimized stealth thermosensitive liposomes improves intratumoral drug delivery and efficacy. *J. Control. Release* **168**, 142–150 (2013).
32. D. An, J. L. Schneller, A. Frassetto, S. Liang, X. Zhu, J. S. Park, M. Theisen, S. J. Hong, J. Zhou, R. Rajendran, B. Levy, R. Howell, G. Besin, V. Presnyak, S. Sabnis, K. E. Murphy-Benenato, E. S. Kumarasinghe, T. Salerno, C. Mihai, C. M. Lukacs, R. J. Chandler, L. T. Guey, C. P. Venditti, P. G. V. Martini, Systemic messenger RNA therapy as a treatment for methylmalonic acidemia. *Cell Rep.* **21**, 3548–3558 (2017).
33. C. Unzu, A. Sampedro, E. Sardh, I. Mauleón, R. E. de Salamanca, J. Prieto, E. Salido, P. Harper, A. Fontanellas, Renal failure affects the enzymatic activities of the three first steps in hepatic heme biosynthesis in the acute intermittent porphyria mouse. *PLOS ONE* **7**, e32978 (2012).
34. D. J. Langford, A. L. Bailey, M. L. Chanda, S. E. Clarke, T. E. Drummond, S. Echols, S. Glick, J. Ingrao, T. Klassen-Ross, M. L. LaCroix-Fralish, L. Matsumiya, R. E. Sorge, S. G. Sotocinal, J. M. Tabaka, D. Wong, A. M. J. M. van den Maagdenberg, M. D. Ferrari, K. D. Craig, J. S. Mogil, Coding of facial expressions of pain in the laboratory mouse. *Nat. Methods* **7**, 447–449 (2010).

Acknowledgments: We are grateful to L. Guembe and S. Arcelus for helpful technical support and A. Sasao, from Kumamoto University, for providing the anti-chloroquine antibody (anti-chloroquine monoclonal antibody—MAC28—is available from A. Sasao of the Kumamoto University, Kumamoto, Japan, under a material transfer agreement—MTA10027—with A.F. and I.S.-M. of the Fundación para la Investigación Médica Aplicada, Pamplona, Spain). T1 and T2 mouse strains were provided by U. A. Meyer (Biozentrum of University of Basel,

Basel, Switzerland). **Funding:** This study was supported by grants from the Spanish Institute of Health Carlos III (FIS) cofinanced by European FEDER funds (PI12/02785 to A.F., PI15/01951 to A.F., PI16/00668 to P.B., PI18/00860 to A.F., PI19/01128 to P.B., and PI21/00546 to A.F.), Spanish Fundación FEDER (FI19010 to A.F.), Spanish Fundación Eugenio Rodríguez Pascual (to A.F.), and Spanish Fundación Mutua Madrileña (to A.F.). No funding from Moderna Inc. supports this work. **Author contributions:** Conception and design: I.S.-M., P.B., and A.F. Experiments and data collections: K.M.C., I.S.-M., D.J., M.M., A.S., M.J.G., M.A., F.C., J.P., P.B., and A.F. Provision of study materials: K.M.C., I.S.-M., D.J., M.M., A.S., M.J.G., M.A., F.C., J.P., P.B., and A.F. Provided the PBGD and ApoAI-PBGD-mRNA messengers: L.J. and P.G.V.M. Analysis and interpretation of the data: K.M.C., I.S.-M., D.J., M.J.G., M.A., F.C., J.P., P.B., and A.F. Statistical expertise: K.M.C., I.S.-M., D.J., and A.F. J.L.L. helped with the confocal microscopy and brain biodistribution of the recombinant protein, and L.J. performed kinetics of hPBGD by LC-MS/MS in livers from AIP mice. Obtaining of funds: P.B. and A.F. Administrative, technical, or logistic support: D.J., M.M., A.S., P.B., and A.F. All authors contributed to review/editing and approved the final submission. **Competing interests:** A.F. reports research funding from Moderna. P.B. reports research funding from Sanofi, Ferring, Hookipa, Moderna, and Bavarian Nordic and speaker honoraria from BMS, MSD, Novartis, Boehringer Ingelheim, and AstraZeneca. L.J. and P.G.V.M. are employees of Moderna Inc. and may hold equities from the company. The other authors declare no competing interests. Additional management/advisory/consulting activities: P.B. reports advisory roles with Ferring, Tusk, and Moderna. A.F., I.S.-M., and P.B. are inventors of patent application no. 16/611,688 "Human porphobilinogen deaminase derived proteins and polynucleotides and uses thereof." Applicant(s): Fundación Para la Investigación Médica Aplicada; international application number: PCT/EP2017/061944; international publication date: 15 November 2018; international publication number: WO2018/206125 A1. **Data and materials availability:** Data are deposited in a standalone Excel file named R2 abc0700 data file S1 and on the website of the Hepatology Department at CIMA-University of Navarra (https://cima.unav.edu/).

Submitted 4 April 2020
Resubmitted 25 June 2021
Accepted 16 November 2021
Published 12 January 2022
10.1126/scitranslmed.abc0700